

# Lipid Rafts: Buffers of Cell Membrane Physical Properties

Jonathan D. Nickels,<sup>\*,†</sup> Micholas Dean Smith,<sup>‡,§</sup> Richard J. Alsop,<sup>||</sup> Sebastian Himbert,<sup>||</sup> Ahmad Yahya,<sup>†</sup> Destini Cordner,<sup>†</sup> Piotr Zolnierczuk,<sup>⊥</sup> Christopher B. Stanley,<sup>#</sup> John Katsaras,<sup>#,∇</sup> Xiaolin Cheng,<sup>○</sup> and Maikel C. Rheinstädter<sup>||</sup>

<sup>†</sup>Department of Chemical and Environmental Engineering, University of Cincinnati, Cincinnati, Ohio 45221, United States

<sup>‡</sup>Center for Molecular Biophysics, Oak Ridge National Laboratory, Oak Ridge, Tennessee 37830, United States

<sup>§</sup>Department of Biochemistry and Cellular and Molecular Biology, University of Tennessee, Knoxville, Tennessee 37996, United States

<sup>||</sup>Department of Physics and Astronomy, McMaster University, Hamilton, ON, L8S 4M1, Canada

<sup>⊥</sup>Jülich Center for Neutron Science, Forschungszentrum Jülich GmbH, Outstation at SNS, Oak Ridge, Tennessee 37830, United States

<sup>#</sup>Large-Scale Structure Group, Oak Ridge National Laboratory, Oak Ridge, Tennessee 37830, United States

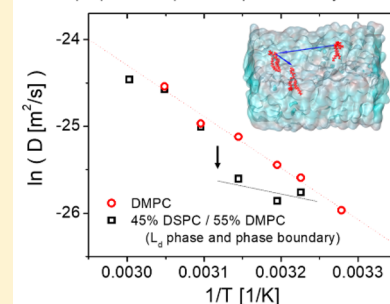
<sup>∇</sup>Shull-Wollen Center, Oak Ridge National Laboratory, Oak Ridge, Tennessee 37830, United States

<sup>○</sup>College of Pharmacy, Medicinal Chemistry & Pharmacognosy Division, The Ohio State University, Columbus, Ohio 43210, United States

## Supporting Information

**ABSTRACT:** Lateral organization of lipids in the cell membrane appears to be an ancient feature of the cell, given the existence of lipid rafts in both eukaryotic and prokaryotic cells. Currently seen as platforms for protein partitioning, we posit that lipid rafts are capable of playing another role: stabilizing membrane physical properties over varying temperatures and other environmental conditions. Membrane composition defines the mechanical and viscous properties of the bilayer. The composition also varies strongly with temperature, with systematic changes in the partitioning of high and low melting temperature membrane components. In this way, rafts function as buffers of membrane physical properties, progressively counteracting environmental changes via compositional changes; i.e., more high melting lipids partition to the fluid phase with increasing temperature, increasing the bending modulus and viscosity, as thermal effects decrease these same properties. To provide an example of this phenomenon, we have performed neutron scattering experiments and atomistic molecular dynamics simulations on a phase separated model membrane. The results demonstrate a buffering effect in both the lateral diffusion coefficient and the bending modulus of the fluid phase upon changing temperature. This demonstration highlights the potentially advantageous stabilizing effect of complex lipid compositions in response to temperature and potentially other membrane destabilizing environmental conditions.

Compositional changes buffer mechanical and viscous properties in phase-separated bilayers



## INTRODUCTION

The emergent picture of the cell membrane as a compositionally rich<sup>1</sup> and laterally organized structure has now largely replaced the classical view of a homogeneous fluid mosaic.<sup>2</sup> The lipid raft hypothesis<sup>3</sup> frequently comes to mind when contextualizing the complex mixture of molecules of lipids, sterols, and membrane proteins found in the cell membrane. The hypothesis<sup>3</sup> invokes the existence of nanoscopic<sup>4,5</sup> and transient<sup>6,7</sup> lateral structures composed of membrane lipids and proteins into distinct domains in the plane of the membrane to facilitate the organization, assembly, and regulation of multimolecular protein complexes. Indeed, this concept provides a compelling rationale for numerous observations relating to complex biological functions such as

membrane trafficking, endocytosis, signal transduction, and other biological processes.<sup>8–11</sup>

Lipid rafts are often thought to be rich in cholesterol and sphingolipids, due to the investigation of these structures in eukaryotic (predominantly mammalian) cell membranes and membrane mimics. This is an incomplete view, as lipid rafts, or raft-like lipid heterogeneities, have been observed in microorganisms such as *B. subtilis*<sup>5,12,13</sup> and *S. aureus*.<sup>14</sup> Beyond offering valuable opportunities for *in vivo* research of rafts, these observations emphasize the deep evolutionary history of complex cell membrane compositions; as stated by López and

**Received:** December 18, 2018

**Revised:** January 2, 2019

**Published:** January 3, 2019

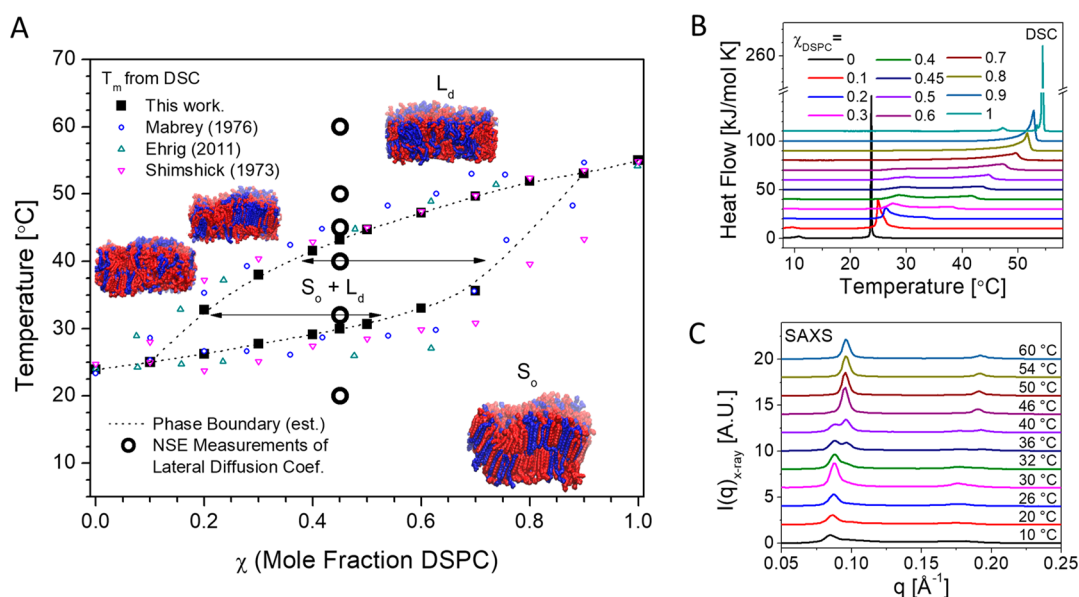


**Figure 1.** DMPC/DSPC mixtures exhibit well-studied phase separation. (A) The phase diagram compiled here from DSC measurements of DMPC/DSPC conforms closely with prior literature.<sup>21–23</sup> (B) DSC thermograms for increasing mole fractions of DSPC. (C) Small angle X-ray scattering (SAXS) also demonstrates phase coexistence, in the 0.45 mol percent of the DSPC system. The bifurcation and shift of the main peak around  $0.09 \text{ \AA}^{-1}$  indicate the coexistence of multiple phases in the temperature range from below 30 to 45 °C.

Kolter,<sup>13</sup> “Their conservation across the two most divergent domains of life argues strongly that these membrane microdomains are an ancient feature of cells”. We concur and note that there are many ways that proteins and lipids mutually interact<sup>15</sup> which involve lipid heterogeneity.

We propose another potential advantage of lateral lipid organization relating to the maintenance of a consistent membrane fluidity and transport and mechanical properties across a range of biologically relevant temperatures. We demonstrate this “buffering” effect by monitoring membrane physical properties as a function of temperature using complementary experimental measurements and all-atom molecular dynamics simulations in a model lipid mixture (1,2-dimyristoyl-*sn*-glycero-3-phosphocholine (DMPC) and 1,2-distearoyl-*sn*-glycero-3-phosphocholine (DSPC)). The significance of the buffering effect emerges from the fact that cells actively regulate their membrane fluidity in response to temperature changes via the membrane composition in what is called the homeoviscous adaptation,<sup>16</sup> a metabolic response that takes both time and energy to implement. Compositional diversity, leading to phase separation, on the other hand provides a rapid buffering effect upon membrane fluidity and other physical properties as the fluid phase becomes progressively enriched in high melting lipid components upon temperature increases.

## RESULTS AND DISCUSSION

This simple model has long been employed in the study of lipid domains<sup>17–20</sup> and has specific experimental advantages in terms of the commercial availability of deuterated lipids. The model “raft” phase is a solid ordered ( $S_o$ ) phase, enriched in DSPC, and the “sea” phase will be represented by the liquid disordered ( $L_d$ ) phase, richer in the lower melting temperature membrane component, DMPC. This is illustrated in Figure 1, where we have used both differential scanning calorimetry, Figure 1B, and small-angle X-ray scattering (multilamellar vesicles in  $H_2O$  at a concentration of 20 mg/mL), Figure 1C,

to show the  $S_o/L_d$  coexistence region between 10 and 90 mol percent DSPC in the temperature range from 25 to 55 °C, in close agreement with previous literature.<sup>21–23</sup>

We chose the 45 mol % mixture of DSPC with DMPC as the model composition with which to monitor the bilayer physical properties. We focus on the  $L_d$  phase, as specific molecular motions of interest exist within our experimental and simulation windows and ordered phases would require far longer simulation times to equilibrate ordered phases accurately.<sup>24</sup> Selected mixtures of DSPC/DMPC were simulated, matching the  $L_d$  composition at the phase boundary (the left-hand boundary in Figure 1). As indicated in Figure 2a, simulations were performed on bilayer patches containing 400 lipid DSPC/DMPC mixtures at temperatures of 45, 50, 55, and 60 °C along with 15, 28, and 36% DSPC/DMPC mixtures at temperatures of 33, 38, and 40 °C, respectively. All-atom molecular dynamics simulations were also performed for membranes consisting entirely of DMPC as a control for a single component bilayer, at temperatures of 25, 30, 35, 40, 45, 50, and 60 °C. Figure 2A and Supporting Tables S1 and S2 summarize the simulation conditions and the simulation lengths. Simulation boxes were constructed using the CHARMM-GUI<sup>25–28</sup> online interface with a total of 400 lipids (200 lipids per leaflet), and all simulations were performed using the GROMACS (2016.3) simulation package.<sup>29</sup> Analysis (using only the last 100 ns) of the simulations was performed using a combination of internal GROMACS utilities, in-house VMD<sup>30</sup> scripts, and the SASSENA<sup>31</sup> molecular dynamics neutron/X-ray analysis software package. Further details of the simulations are provided in the Supporting Information.<sup>25–38</sup>

The area per lipid, or APL, is an important structural parameter which, in combination with molecular volume and elemental composition (and hydration state), provides a description of the z-profile and bilayer thickness of lipid bilayers.<sup>39</sup> We have obtained the APL from our simulations. In a single component bilayer, the APL increases rapidly upon

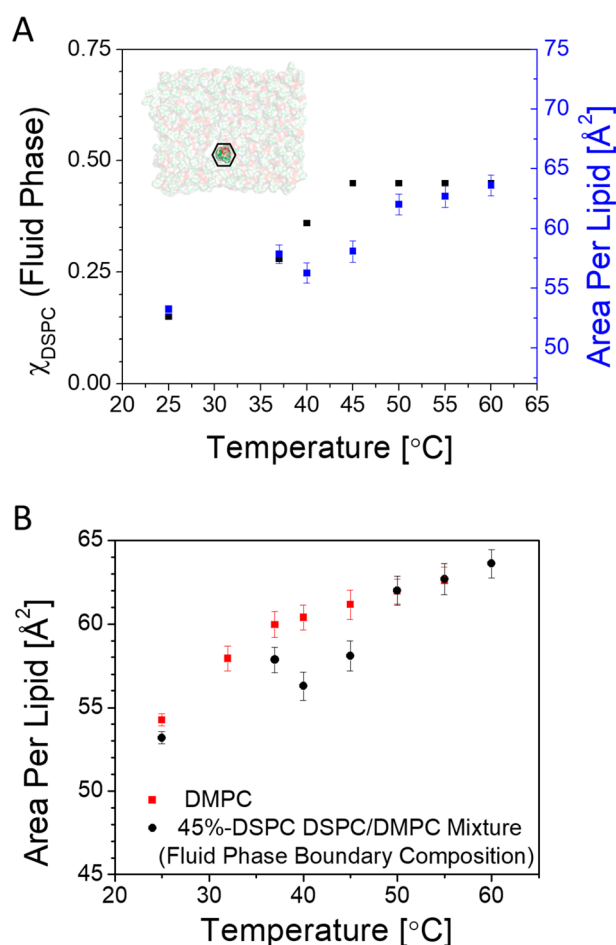


**Figure 2.** MD simulations were performed on a series of DMPC/DSPC lipid mixtures matching the fluid phase component for a range of temperatures from 25 to 60 °C. (A) The mole fraction of DSPC in the fluid phase increases with increasing temperature, shown on the left axis, while the right axis shows the area per lipid for the fluid phase composition at each temperature. (B) The area per lipid, compared to a single component DMPC bilayer, increases more gradually at the fluid phase boundary of the  $L_d/S_o$  coexistence regime.

melting to the fluid phase and then increases in a roughly linear temperature dependence, as described by the thermal expansion coefficient. Indeed, this is what we observe for DMPC bilayers in Figure 2B, where the APL for DMPC

rapidly increases near the melting temperature, before continuing to increase linearly. The 0.45 mole fraction DSPC/DMPC systems show a similar linear increase above the phase miscibility temperature. However, below 45 °C, there appears to be a plateau in the area per lipid for the  $L_d$  composition. This plateau in APL is a demonstration of the buffering of membrane structure through the phase coexistence temperature range by the continuous addition of the higher melting temperature component to the  $L_d$  phase. The structure of the bilayer matters greatly for the proper functioning of membrane proteins.<sup>40–42</sup> Indeed, the hydrophobic thickness matching is thought to be one of the driving forces for partitioning of membrane proteins between the raft and “sea” phases.<sup>3</sup>

Given the stabilizing effect in the APL, we anticipate a similar effect in the elastic and viscous properties of the bilayer. In the liquid disordered state, the membrane behaves as a two-dimensional fluid which can be characterized by physical parameters such as the lateral diffusion coefficient of the constituent lipids. Fundamental molecular relaxations occurring in the acyl region govern diffusion through the viscosity.<sup>43</sup> The same relaxations govern the elastic properties of the bilayer, such as the bending modulus through the area compressibility.<sup>44</sup> The frequency of these fundamental molecular relaxations increases rapidly with increasing temperature following an Arrhenius dependence,<sup>45</sup> suggesting that the viscosity and bending moduli will decrease rapidly, while the lateral diffusion coefficient will increase rapidly. In Figure 3A, we plot the lateral diffusion coefficient evaluated from MD simulations for both the single component DMPC bilayer and the  $L_d$  phase boundary of the 45% DSPC/55% DMPC system. The lateral diffusion coefficient was obtained by a linear fitting of the slope of the lateral ( $x/y$ ) mean-squared displacement of the phosphate atoms from the lipid head-groups. In the single component DMPC bilayer, we observe a monotonic increase as a function of temperature, as expected for a pure DMPC bilayer. In the coexisting system on the other hand, there is a plateau in the temperature range of phase coexistence, comparable to that seen for the APL.

In Figure 3A, a plateau in the values of the lateral diffusion coefficient,  $D$ , is apparent for the 45% DSPC/55% DMPC system along the  $L_d$  phase boundary, in agreement with experimental measurement of the lateral diffusion coefficient discussed later in this work. The solid ordered region would

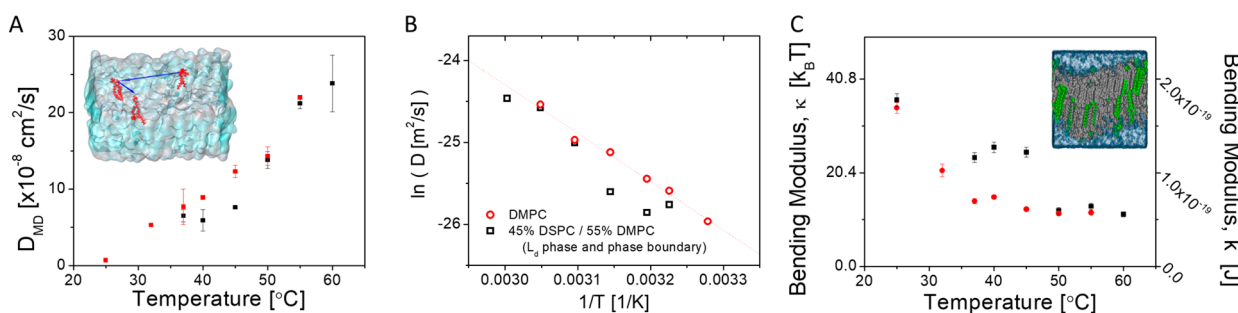


**Figure 3.** Lateral diffusion coefficient and bending modulus obtained from MD simulations for DMPC and DMPC/DSPC mixtures representing the fluid phase boundary composition. (A) The lateral diffusion coefficient,  $D$ , exhibits a plateau in  $D$  between 35 and 45 °C. (B) An Arrhenius plot reveals a  $1/T$  dependence in the single component bilayer, while the data from the phase boundary compositions demonstrates the added effect of compositional changes. (C) The bending modulus exhibits a steady decrease as a function of temperature for the single component bilayer and a plateau for the temperature range of phase coexistence. The plateau in both physical parameters within the  $S_o-L_d$  coexistence regime illustrates the thermal buffering effect of phase separated lipid bilayers.

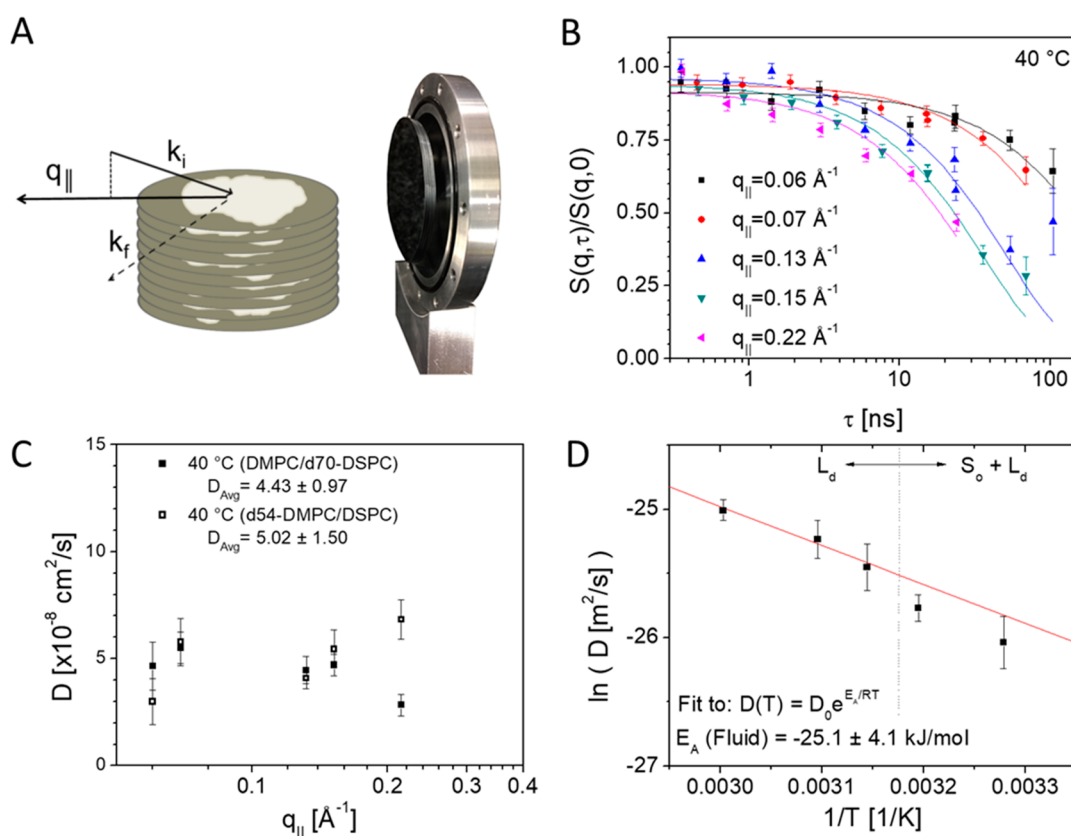


**Figure 4.** Lateral diffusion was measured using neutron spin echo spectroscopy. (A) Experiments were conducted on  $D_2O$  hydrated, supported lipid bilayer stacks composed aligned such that the scattering wave vector was parallel,  $q_{||}$ , with respect to the plane of the lipid bilayers. (B) NSE measures the dynamic structure factor,  $S(q_{||}, \tau)/S(q_{||}, 0)$ , over a range of scattering wave vectors,  $q$ , and Fourier times,  $\tau$ , shown here for 40 °C. Solid lines are a fit of a single exponential decay to the data. (C) The lateral diffusion coefficient,  $D$ , is obtained from the decay constants,  $\Gamma(q)$ , and the probe length associated with the scattering wave vector,  $q$ , as,  $D = (2\pi)^2 \Gamma/q^2$ . In this  $||$  configuration, the decreasing values of  $S(q, \tau)/S(q, 0)$  with increasing  $\tau$  are related to diffusional motions in the plane of the bilayer; confirmed via the  $q^2$  dependence implied by a consistent value of  $D$  as a function of  $q$ . The inverse deuteration scheme (DSPC/*d*54-DMPC) demonstrates the observed value of  $D$  is independent of which lipid is labeled, consistent with prior reports.<sup>46</sup> (D)  $D$  was measured as a function of temperature, plotted here in Arrhenius format. The deviation from the Arrhenius temperature dependence below the miscibility temperature is consistent with the plateau observed in our MD simulations and the proposed buffering effect.

exhibit a rapid reduction in the lateral diffusion coefficient.<sup>46</sup> An Arrhenius plot of  $D$  from the simulations is shown in Figure 3B. A linear trend is observed for DMPC, from which an activation energy of 48.7 kJ/mol can be estimated, slightly higher when compared to experimentally determined values but clearly demonstrating the expected Arrhenius temperature dependence of a single component lipid bilayer. The plateau region 45% DSPC/55% DMPC system along the  $L_d$  phase boundary is visible in this presentation as a dislocation and region of more shallow slope. This deviation quantitatively demonstrates the stabilizing effect of compositional changes upon the lateral diffusion coefficient.

The bending modulus of the fluid phase boundary compositions was also investigated. It describes the out-of-plane flexibility of membranes and is an important physical parameter for the fusion of vesicles and bilayer stability.<sup>47</sup> This is also important for the case of laterally heterogeneous bilayers, where curvature coupling<sup>48</sup> and efficient dissipation of thermal energy via thermal fluctuations<sup>49</sup> are potential driving forces for phase separation. Here, the bending moduli were also obtained from the simulation trajectories using a VMD/tcl implementation of the splay/tilt based method proposed by Khelashvili et al.<sup>38</sup> The resulting values of the bending modulus have been plotted in Figure 3C.

The bending modulus for the single component DMPC system shows a steadily decreasing value as a function of increasing temperature, while the liquid phase boundary of the 45% DSPC/55% DMPC demonstrates a plateau in the phase coexistence regime between  $\sim 30$  and 45 °C. This data is consistent with the argument of a thermal buffering effect. It is not unexpected that the progressively increasing content of DSPC in the fluid phase would counteract the effects of increasing temperature. It is well-known that longer tail length increases the bending modulus<sup>50</sup> while the increase in temperature increases the frequency of fundamental molecular relaxations following an Arrhenius dependence.<sup>45</sup> Thickness fluctuations are another out of plane dynamical mode that show a strong temperature dependence in single component systems. A decoupling of the relaxation times of thickness fluctuations from temperature was reported for DMPC/DSPC systems, seemingly consistent with our results.<sup>20</sup>

Experimental observations of the lateral diffusion coefficient have also been obtained. Neutron spin echo (NSE) spectroscopy was performed on aligned, supported lipid bilayers at 45:55 mol percent *d*70-DSPC/DMPC, analogous to the simulations. The tail deuterated version of DSPC (*d*70-DMPC) was used to enhance the scattering signal. NSE is being utilized here as a coherent inelastic neutron scattering

technique by which we can observe collective motions of the bilayer structure and/or the constituent lipids. The aligned model membranes were prepared on undoped silicon substrates by deposition of dissolved lipids from 1:1 chloroform:trifluoroethanol.<sup>51</sup> Solvent was allowed to evaporate and dried under a vacuum. Samples were then hydrated with D<sub>2</sub>O to 1.1:1 hydration by mass (an equivalent of 1:1 hydration using H<sub>2</sub>O) and annealed in a sealed container at 60 °C for 8 h. As shown in Figure 4A, a “stack” of 10 such aligned lipid bilayer samples were prepared to arrive at approximately 50 mg of lipid content which were then sealed in an aluminum sample holder and mounted on the instrument.

Observations were made in the plane of the bilayer by aligning the scattering wave vector,  $\mathbf{Q}$ , parallel to the direction of sample alignment, Figure 4A. Diffraction measurements, see Figure S2, demonstrate the scattering from both a parallel,  $q_{\parallel}$ , and perpendicular,  $q_{\perp}$ , geometry, with the orientations confirmed via a rocking curve. The perpendicular orientation results in scattering dominated by the transverse structural contributions such as the intermembrane distance. We mitigate any spurious contributions from transverse structure by performing our NSE measurements at  $q$ -values which are less influenced by out of plane contributions. The observed quantity of NSE measurements, shown in Figure 4B, is the intermediate scattering function,  $S(q, \tau)/S(q, 0)$ . It reflects the fraction of pair correlations still in existence after a given time interval,  $\tau$ , for a given length scale (equal to  $2\pi$  divided by the scattering wave vector  $q$ ). This length scale is systematically varied by measuring  $q$ -values from  $0.06 \text{ \AA}^{-1} < q < 0.22 \text{ \AA}^{-1}$ , corresponding to distances smaller than domain sizes.<sup>52</sup>  $S(q, \tau)/S(q, 0)$  typically takes the shape of an exponential decay as a lower number of correlations persist as longer times are probed, and similarly as longer length scales are probed. Observations were made over the time range from 100 ps to 100 ns. A range of temperatures—20, 32, 40, 45, 50, and 60 °C—were used to probe the temperature dependence of the lateral diffusion. The dynamics of the solid ordered phase will be outside of our observational window for experiments using the neutron spin echo technique (NSE).

The data can be modeled as an exponential decay at each  $q$ -value where the resulting decay constants,  $\Gamma(q)$ , reflect the average relaxation time for a given scattering wave vector, or length scale of the molecular motions. The diffusion coefficient is obtained from the decay constant multiplied by the square of the length scale probed ( $D = \Gamma(q) \times l^2$ , where  $l = 2\pi/q$ ). In Figure 4C, we plot  $D$  as a function of  $q$  at 40 °C; the constant value of  $D$  as a function of  $q$  illustrates the  $q^2$  dependence (i.e., diffusive nature) of these motions. A reversed case of d54-DMPC/DSPC was also used as a control for one temperature (40 °C), showing that the dynamics observed were not specific to either lipid but to the fluid phase. This is consistent with pulsed field gradient NMR experiments.<sup>46</sup>

The experimental observations of the diffusion coefficient were performed as a function of temperature. We plot the natural logarithm of the observed relaxation time against the reciprocal temperature in Figure 4D to illustrate both the Arrhenius dependence seen above the miscibility temperature and the deviation from that trend upon crossing the phase coexistence boundary. This presentation emphasizes the Arrhenius temperature dependence of the fully mixed membrane at high temperature as a straight line, as expected due to the Arrhenius temperature dependence of the viscosity of fluid phase membranes.<sup>53</sup> For the fully mixed fluid phase at

temperatures above the phase coexistence regime, the activation energy for this process was found to be  $25.2 \pm 4.1$  kJ/mol, in good agreement with the value of  $\sim 27$  kJ/mol reported in the literature,<sup>53</sup> though reported values do vary substantially between experimental methods and lipid measured.<sup>54,55</sup>

At temperatures coinciding with the temperature range of phase separation ( $< 45$  °C), there is a deviation from the Arrhenius temperature dependence. Similar to what has been observed in the simulations, there is an apparent change in the effective activation energy of the structural relaxations which govern viscosity<sup>56</sup> and consequently in the lateral diffusion.<sup>43</sup> Lipid phase separation is driven by the balance of enthalpic gain and entropic penalty (along with other effects such as curvature matching, dipolar orientations, and bending moduli distribution).<sup>57</sup> It is the competition between this thermodynamic cost of lipid exchange (i.e., partitioning progressively larger content of high melting temperature lipid (DSPC) in the fluid phase) and the structural relaxation rate, which is the physical origin of the observed stability of the lateral diffusion coefficient, area per lipid, and bending modulus.

## CONCLUSIONS

The classical view of a homogeneous fluid mosaic<sup>2</sup> cell membrane has evolved into a vision of a structurally complex<sup>58</sup> and compositionally diverse<sup>59</sup> membrane that is still being unraveled in terms of emergent structures, biophysics, and biochemistry. In this work, we have put forward the hypothesis that lipid rafts, or lateral lipid heterogeneities rich in high melting lipids, function not only as functional platforms for membrane proteins but also as reservoirs of high melting lipids that act as thermal buffers of membrane physical properties. Our experimental observations and MD simulations of a simple model membrane demonstrate this concept. We can speculate that this buffering effect provides a biological advantage by maintaining a more consistent physical environment than would be possible with single component membranes which undergo rapid phase transitions. Such changes in a single phase bilayer could potentially arrest membrane associated biochemistry by changing protein function or localization. Our hypothesis suggests that complex membrane compositions offer a simple buffering effect upon membrane physical properties based on the thermodynamics of phase separation which is far more responsive than the metabolic response in composition described by the homeoviscous adaptation.<sup>16</sup> The purely physical advantage of lipid rafts might be envisioned at the ancient origins of lipid rafts, providing a platform which later found use in “functional” activities which are seen as the role of lipid rafts today.

## ASSOCIATED CONTENT

### Supporting Information

The Supporting Information is available free of charge on the ACS Publications website at DOI: 10.1021/acs.jpcc.8b12126.

Supporting Figures 1 and 2, Supporting Tables 1 and 2, and details describing the methodology and analysis of the MD simulations (PDF)

## AUTHOR INFORMATION

### Corresponding Author

\*E-mail: Jonathan.Nickels@uc.edu.

ORCID 

Jonathan D. Nickels: 0000-0001-8351-7846

Nicholas Dean Smith: 0000-0002-0777-7539

Richard J. Alsop: 0000-0003-0563-0063

Christopher B. Stanley: 0000-0002-4226-7710

Xiaolin Cheng: 0000-0002-7396-3225

Maikel C. Rheinstädter: 0000-0002-0558-7475

## Notes

The authors declare no competing financial interest.

## ACKNOWLEDGMENTS

The authors would like to acknowledge the extraordinary technical support of Malcolm Cochran. R.J.A., S.H., and M.C.R. were supported by the Natural Sciences and Engineering Research Council of Canada (NSERC) and McMaster University. This research used resources of the Oak Ridge Leadership Computing Facility at the Oak Ridge National Laboratory, which is supported by the Office of Science of the U.S. Department of Energy under Contract No. DE-AC05-00OR22725. This research also used resources of the Ohio Supercomputer Center (OSC) provided to X.C. This research also used resources of the Compute and Data Environment for Science (CADES) provided to M.D.S. M.D.S. was partially supported by ORNL Laboratory Directed R&D (LDRD) project 8294. J.K. is supported through the Scientific User Facilities Division of the Department of Energy (DOE) Office of Science, sponsored by the Basic Energy Science (BES) Program, DOE Office of Science, under Contract No. DEAC05-00OR22725. This research used resources at the Spallation Neutron Source, a DOE Office of Science User Facility operated by the Oak Ridge National Laboratory.

## REFERENCES

- (1) Shevchenko, A.; Simons, K. Lipidomics: Coming to Grips with Lipid Diversity. *Nat. Rev. Mol. Cell Biol.* **2010**, *11*, 593–598.
- (2) Singer, S. J.; Nicolson, G. L. The Fluid Mosaic Model of the Structure of Cell Membranes. *Science* **1972**, *175*, 720–731.
- (3) Simons, K.; Ikonen, E. Functional Rafts in Cell Membranes. *Nature* **1997**, *387*, 569–572.
- (4) Topozini, L.; Meinhardt, S.; Armstrong, C. L.; Yamani, Z.; Kučerka, N.; Schmid, F.; Rheinstädter, M. C. Structure of Cholesterol in Lipid Rafts. *Phys. Rev. Lett.* **2014**, *113*, 228101.
- (5) Nickels, J. D.; Chatterjee, S.; Stanley, C. B.; Qian, S.; Cheng, X.; Myles, D. A.; Standaert, R. F.; Elkins, J. G.; Katsaras, J. The In Vivo Structure of Biological Membranes and Evidence for Lipid Domains. *PLoS Biol.* **2017**, *15*, e2002214.
- (6) Lingwood, D.; Simons, K. Lipid Rafts as a Membrane-Organizing Principle. *Science* **2010**, *327*, 46–50.
- (7) Mukherjee, S.; Maxfield, F. R. Membrane Domains. *Annu. Rev. Cell Dev. Biol.* **2004**, *20*, 839–866.
- (8) Allen, J. A.; Halverson-Tamboli, R. A.; Rasenick, M. M. Lipid Raft Microdomains and Neurotransmitter Signalling. *Nat. Rev. Neurosci.* **2007**, *8*, 128–140.
- (9) Shaw, A. S. Lipid Rafts: Now You See Them, Now You Don't. *Nat. Immunol.* **2006**, *7*, 1139–1142.
- (10) Simons, K.; Ehehalt, R. Cholesterol, Lipid Rafts, and Disease. *J. Clin. Invest.* **2002**, *110*, 597–603.
- (11) Simons, K.; Toomre, D. Lipid Rafts and Signal Transduction. *Nat. Rev. Mol. Cell Biol.* **2000**, *1*, 31–39.
- (12) Kawai, F.; Shoda, M.; Harashima, R.; Sadaie, Y.; Hara, H.; Matsumoto, K. Cardiolipin Domains in *Bacillus subtilis* Marburg Membranes. *J. Bacteriol.* **2004**, *186*, 1475–1483.
- (13) López, D.; Kolter, R. Functional Microdomains in Bacterial Membranes. *Genes Dev.* **2010**, *24*, 1893–1902.
- (14) García-Fernández, E.; Koch, G.; Wagner, R. M.; Fekete, A.; Stengel, S. T.; Schneider, J.; Mielich-Süss, B.; Geibel, S.; Markert, S. M.; Stigloher, C. Membrane Microdomain Disassembly Inhibits MRSA Antibiotic Resistance. *Cell* **2017**, *171*, 1354–1367.e20.
- (15) Sprong, H.; van der Sluijs, P.; van Meer, G. How Proteins Move Lipids and Lipids Move Proteins. *Nat. Rev. Mol. Cell Biol.* **2001**, *2*, 504.
- (16) Sinensky, M. Homeoviscous Adaptation—A Homeostatic Process that Regulates the Viscosity of Membrane Lipids in *Escherichia coli*. *Proc. Natl. Acad. Sci. U. S. A.* **1974**, *71*, 522–525.
- (17) Knoll, W.; Schmidt, G.; Sackmann, E.; Ibel, K. Critical Demixing in Fluid Bilayers of Phospholipid Mixtures. A Neutron Diffraction Study. *J. Chem. Phys.* **1983**, *79*, 3439–3442.
- (18) Gliss, C.; Clausen-Schaumann, H.; Günther, R.; Odenbach, S.; Randl, O.; Bayerl, T. M. Direct Detection of Domains in Phospholipid Bilayers by Grazing Incidence Diffraction of Neutrons and Atomic Force Microscopy. *Biophys. J.* **1998**, *74*, 2443–2450.
- (19) Sugar, I. P.; Michonova-Alexova, E.; Chong, P. L.-G. Geometrical Properties of Gel and Fluid Clusters in DMPC/DSPC Bilayers: Monte Carlo Simulation Approach using a Two-State Model. *Biophys. J.* **2001**, *81*, 2425–2441.
- (20) Ashkar, R.; Nagao, M.; Butler, P. D.; Woodka, A. C.; Sen, M. K.; Koga, T. Tuning Membrane Thickness Fluctuations in Model Lipid Bilayers. *Biophys. J.* **2015**, *109*, 106–112.
- (21) Ehrig, J.; Petrov, E. P.; Schwille, P. Near-critical Fluctuations and Cytoskeleton-assisted Phase Separation Lead to Subdiffusion in Cell Membranes. *Biophys. J.* **2011**, *100*, 80–89.
- (22) Mabrey, S.; Sturtevant, J. M. Investigation of Phase Transitions of Lipids and Lipid Mixtures by Sensitivity Differential Scanning Calorimetry. *Proc. Natl. Acad. Sci. U. S. A.* **1976**, *73*, 3862–3866.
- (23) Shimshick, E. J.; McConnell, H. M. Lateral Phase Separation in Phospholipid Membranes. *Biochemistry* **1973**, *12*, 2351–2360.
- (24) Sodt, A. J.; Sandar, M. L.; Gawrisch, K.; Pastor, R. W.; Lyman, E. The Molecular Structure of the Liquid-Ordered phase of Lipid Bilayers. *J. Am. Chem. Soc.* **2014**, *136*, 725–732.
- (25) Jo, S.; Kim, T.; Iyer, V. G.; Im, W. CHARMM-GUI: A Web-Based Graphical User Interface for CHARMM. *J. Comput. Chem.* **2008**, *29*, 1859–65.
- (26) Wu, E. L.; Cheng, X.; Jo, S.; Rui, H.; Song, K. C.; Davila-Contreras, E. M.; Qi, Y. F.; Lee, J. M.; Monje-Galvan, V.; Venable, R. M.; Klauda, J. B.; Im, W. CHARMM-GUI Membrane Builder Toward Realistic Biological Membrane Simulations. *J. Comput. Chem.* **2014**, *35*, 1997–2004.
- (27) Lee, J.; Cheng, X.; Swails, J. M.; Yeom, M. S.; Eastman, P. K.; Lemkul, J. A.; Wei, S.; Buckner, J.; Jeong, J. C.; Qi, Y. F.; Jo, S.; Pande, V. S.; Case, D. A.; Brooks, C. L.; MacKerell, A. D.; Klauda, J. B.; Im, W. CHARMM-GUI Input Generator for NAMD, GROMACS, AMBER, OpenMM, and CHARMM/OpenMM Simulations Using the CHARMM36 Additive Force Field. *J. Chem. Theory Comput.* **2016**, *12*, 405–413.
- (28) Jo, S.; Cheng, X.; Lee, J.; Kim, S.; Park, S. J.; Patel, D. S.; Beaven, A. H.; Lee, K. I.; Rui, H.; Park, S.; Lee, H. S.; Roux, B.; MacKerell, A. D.; Klauda, J. B.; Qi, Y. F.; Im, W. CHARMM-GUI 10 Years for Biomolecular Modeling and Simulation. *J. Comput. Chem.* **2017**, *38*, 1114–1124.
- (29) Abraham, M. J.; Murtola, T.; Schulz, R.; Páll, S.; Smith, J. C.; Hess, B.; Lindahl, E. GROMACS: High Performance Molecular Simulations Through Multi-Level Parallelism from Laptops to Supercomputers. *SoftwareX* **2015**, *1–2*, 19–25.
- (30) Humphrey, W.; Dalke, A.; Schulten, K. VMD: Visual Molecular Dynamics. *J. Mol. Graphics* **1996**, *14*, 33–38.
- (31) Lindner, B.; Smith, J. C. Sassena - X-ray and Neutron Scattering Calculated from Molecular Dynamics Trajectories Using Massively Parallel Computers. *Comput. Phys. Commun.* **2012**, *183*, 1491–1501.
- (32) Berendsen, H. J. C.; Postma, J. P. M.; Vangunsteren, W. F.; Dinola, A.; Haak, J. R. Molecular-Dynamics with Coupling to an External Bath. *J. Chem. Phys.* **1984**, *81*, 3684–3690.

- (33) Hess, B.; Bekker, H.; Berendsen, H. J. C.; Fraaije, J. G. E. M. LINCS: A Linear Constraint Solver for Molecular Simulations. *J. Comput. Chem.* **1997**, *18*, 1463–1472.
- (34) Hoover, W. G. Canonical Dynamics - Equilibrium Phase-Space Distributions. *Phys. Rev. A: At., Mol., Opt. Phys.* **1985**, *31*, 1695–1697.
- (35) Nose, S. A Molecular-Dynamics Method for Simulations in the Canonical Ensemble. *Mol. Phys.* **1984**, *52*, 255–268.
- (36) Nose, S.; Klein, M. L. Constant Pressure Molecular-Dynamics for Molecular-Systems. *Mol. Phys.* **1983**, *50*, 1055–1076.
- (37) Parrinello, M.; Rahman, A. Polymorphic Transitions in Single-Crystals - a New Molecular-Dynamics Method. *J. Appl. Phys.* **1981**, *52*, 7182–7190.
- (38) Khelashvili, G.; Kollmitzer, B.; Heftberger, P.; Pabst, G.; Harries, D. Calculating the Bending Modulus for Multicomponent Lipid Membranes in Different Thermodynamic Phases. *J. Chem. Theory Comput.* **2013**, *9*, 3866–3871.
- (39) Nagle, J. F.; Tristram-Nagle, S. Structure of Lipid Bilayers. *Biochim. Biophys. Acta, Rev. Biomembr.* **2000**, *1469*, 159–195.
- (40) Lee, A. G. How Lipids Affect the Activities of Integral Membrane Proteins. *Biochim. Biophys. Acta, Biomembr.* **2004**, *1666*, 62–87.
- (41) Dumas, F.; Chantal, L. M.; Jean-François, T. Is the Protein/Lipid Hydrophobic Matching Principle Relevant to Membrane Organization and Functions? *FEBS Lett.* **1999**, *458*, 271–277.
- (42) Jensen, M. Ø.; Mouritsen, O. G. Lipids do Influence Protein Function—The Hydrophobic Matching Hypothesis Revisited. *Biochim. Biophys. Acta, Biomembr.* **2004**, *1666*, 205–226.
- (43) Saffman, P.; Delbrück, M. Brownian Motion in Biological Membranes. *Proc. Natl. Acad. Sci. U. S. A.* **1975**, *72*, 3111–3113.
- (44) Nagao, M.; Kelley, E. G.; Ashkar, R.; Bradbury, R.; Butler, P. D. Probing Elastic and Viscous Properties of Phospholipid Bilayers Using Neutron Spin Echo Spectroscopy. *J. Phys. Chem. Lett.* **2017**, *8*, 4679–4684.
- (45) Wu, Y.; Stefl, M.; Olzyska, A.; Hof, M.; Yahioğlu, G.; Yip, P.; Casey, D. R.; Ces, O.; Humpolickova, J.; Kuimova, M. K. Molecular Rheometry: Direct Determination of Viscosity in Lo and Ld Lipid Phases via Fluorescence Lifetime Imaging. *Phys. Chem. Chem. Phys.* **2013**, *15*, 14986–14993.
- (46) Orådd, G.; Westerman, P. W.; Lindblom, G. Lateral Diffusion Coefficients of Separate Lipid Species in a Ternary Raft-Forming Bilayer: A Pfg-NMR Multinuclear Study. *Biophys. J.* **2005**, *89*, 315–320.
- (47) Huttner, W. B.; Zimmerberg, J. Implications of Lipid Microdomains for Membrane Curvature, Budding and Fission: Commentary. *Curr. Opin. Cell Biol.* **2001**, *13*, 478–484.
- (48) Schick, M. Membrane Heterogeneity: Manifestation of a Curvature-Induced Microemulsion. *Phys. Rev. E* **2012**, *85*, 031902.
- (49) Nickels, J. D.; Cheng, X.; Mostofian, B.; Stanley, C.; Lindner, B.; Heberle, F. A.; Perticaroli, S.; Feygenson, M.; Egami, T.; Standaert, R. F.; Smith, J. C.; Myles, D. A. A.; Ohl, M.; Katsaras, J. Mechanical Properties of Nanoscopic Lipid Domains. *J. Am. Chem. Soc.* **2015**, *137*, 15772–15780.
- (50) Rawicz, W.; Olbrich, K.; McIntosh, T.; Needham, D.; Evans, E. Effect of Chain Length and Unsaturation on Elasticity of Lipid Bilayers. *Biophys. J.* **2000**, *79*, 328–339.
- (51) Tristram-Nagle, S. A. Preparation of Oriented, Fully Hydrated Lipid Samples for Structure Determination Using X-Ray Scattering. *Methods Mol. Biol.* **2007**, *400*, 63–75.
- (52) Sankaram, M.; Marsh, D.; Thompson, T. Determination of Fluid and Gel Domain Sizes in Two-Component, Two-Phase Lipid Bilayers. An Electron Spin Resonance Spin Label Study. *Biophys. J.* **1992**, *63*, 340–349.
- (53) Wu, E.; Jacobson, K.; Papahadjopoulos, D. Lateral Diffusion in Phospholipid Multibilayers Measured by Fluorescence Recovery after Photobleaching. *Biochemistry* **1977**, *16*, 3936–3941.
- (54) Vaz, W. L.; Clegg, R. M.; Hallmann, D. Translational Diffusion of Lipids in Liquid Crystalline Phase Phosphatidylcholine Multibilayers. A Comparison of Experiment with Theory. *Biochemistry* **1985**, *24*, 781–786.
- (55) Gaede, H. C.; Gawrisch, K. Lateral Diffusion Rates of Lipid, Water, and a Hydrophobic Drug in a Multilamellar Liposome. *Biophys. J.* **2003**, *85*, 1734–1740.
- (56) Angell, C. Relaxation in Liquids, Polymers and Plastic Crystals—Strong/Fragile Patterns and Problems. *J. Non-Cryst. Solids* **1991**, *131*, 13–31.
- (57) Seul, M.; Andelman, D. Domain Shapes and Patterns: The Phenomenology of Modulated Phases. *Science* **1995**, *267*, 476–483.
- (58) Nickels, J. D.; Smith, J. C.; Cheng, X. Lateral Organization, Bilayer Asymmetry, and Inter-Leaflet Coupling of Biological Membranes. *Chem. Phys. Lipids* **2015**, *192*, 87–99.
- (59) Nickels, J. D.; Chatterjee, S.; Mostofian, B.; Stanley, C. B.; Ohl, M.; Zolnierczuk, P.; Schulz, R.; Myles, D. A.; Standaert, R. F.; Elkins, J.; Cheng, X.; Katsaras, J. The Bacillus Subtilis Lipid Extract, A Branched-Chain Fatty Acid Model Membrane. *J. Phys. Chem. Lett.* **2017**, *8*, 4214–4217.